Linear Conservative Finite Volume Element Schemes for the Gardner Equation

Jin-Liang Yan and Liang-Hong Zheng

***Abstract*—In this paper, a linear implicit energy-preserving and a linear explicit momentum-preserving finite volume element scheme are proposed for the Gardner equation. The proposed schemes are derived by using the discrete variational derivative method (DVDM) in time and the finite volume element method (FVEM) in space. The conservative properties and the linear stability of the proposed schemes are analyzed. In particular, the proposed methods are compared with a nonlinear Crank-Nicolson FVEM and a third-order Runge-Kutta FVEM in terms of accuracy, CPU time and conservative properties.**

***Index Terms*—Energy, Momentum, Discrete variational derivative method, Finite volume element method, Gardner equation.**

I. Introduction

THIS section is divided into the following parts:

- The introduction to the nonlinear Gardner equation;
- The DVDM and the FVEM;
- The literature review and a brief introduction to the current work.

A. Nonlinear Gardner equation

The nonlinear Gardner equation

$$u_t + 2\alpha u u_x - 3\beta u^2 u_x + \mu u_{xxx} = 0, a \le x \le b, t > 0, \quad (1)$$

where $u(x,t)$ is the amplitude of the wave and α, β and μ are positive constants. It possesses solitary wave solutions that have been identified in a large variety of wave(see [1], [2]). The equation includes two nonlinear terms and a dispersion term, the competition of three terms constitutes the main interest [2]. Particularly, when $\beta = 0$, we obtain the Korteweg-de Vries (KdV) equation, and when $\alpha = 0$, we again obtain the modified Korteweg-de Vries (mKdV) equation. Thus, the Gardner equation is also named KdV-mKdV equation. Moreover, this equation has an infinite number of conservation laws [3], and the first three of them are

$$M(t) = \int_a^b u(x,t)\,dx,$$
$$K(t) = \frac{1}{2}\int_a^b u(x,t)^2\,dx,$$
$$J(t) = \int_a^b \left[\frac{\alpha}{3}u(x,t)^3 - \frac{\beta}{4}u(x,t)^4 - \frac{\mu}{2}u_x(x,t)^2\right]dx,$$

which are respectively named mass, momentum, and energy.

The ability of a numerical scheme to reproduce these quantities is extremely important, most particularly when they are conservative. Some applications of this model can be found in the hydrodynamics [4], plasma physics [5], and so on.

B. The DVDM and the FVEM

As is said in [6], schemes that conserve the first integrals or generalized geometric structure have been shown to be useful when studying the long time behavior of dynamical systems. These schemes sometimes called geometric or structure preserving integrators [7].

The DVDM [8] is a class of important structure-preserving method that can retain the conservative/dissipative properties of the original partial differential equations. Up to now, it has been applied to many conservative or dissipative partial differential equations (PDEs)(see [9]–[11]). In particular, Koide and Furihata [9] proposed four conservative difference schemes for the regularized long wave equation. Matsuo and Furihata [10] extended the general studies to complex-valued PDEs. Miyatake and Matsuo [12] proposed a general framework for constructing energy dissipative or conservative Galerkin schemes for time dependent PDEs. Yan [13] developed a class of energy-preserving FVEM for the KdV equation.

The FVEM, as a type of important numerical tool for solving differential equations (see [11], [14]–[16]), has a long history. This method is also known as a box method in early references [17], or known as a generalized difference method in China [18]. The method has been widely used in several engineering fields, such as fluid mechanics, heat and mass transfer and petroleum engineering. Perhaps the most important property of the FVEM is that it can preserve the conservation laws (mass, momentum and heat flux) on each computational cell. This important property, combined with adequate accuracy and ease of implementation, has attracted more people to do research in this field. For example, Cai [14] developed the general error analysis framework for the FVEM. Yan [19] proposed a class of two-grid FVEM for the Sobolev equation. Wang [16] proposed an energy-preserving finite volume element method for the improved Boussinesq equation. Further, Yan [11] developed a class of

Manuscript received April 21,2018; revised July 11, 2018. This work was supported in part by the National Natural Science of China(Grant NO. 11861047), Foundation Jiangsu Key Laboratory for NSLSCS (Grant No. 201804), PhD Start-up Fund of Wuyi University (Grant No. YJ201702), the Education Foundation of Fujian Province for Young Teachers(Grant No. JA14319, NO. JAT160519), Natural Science Foundation of Fujian Province(Grant No. 2016J01682).

Jin-Liang Yan is with the department of Mathematics and Computer, Wuyi University, Wuyi Shan, Fujian, 354300, China, e-mail: yanjinliang3333@163.com.

Liang-Hong Zheng is with the department of Information and Computer Technology, No 1 middle school of Nanping, Nanping, Fujian, 353000, China. e-mail: 413845939@qq.com.

nonlinear energy-preserving and momentum-preserving finite volume element scheme for the mKdV equation, and so on. In this work, we will develop a class of linear conservative FVEM based on the DVDM and the FVEM. Generally, the main merits of the proposed methods can be summarized as follows:

- They can precisely conserve the conservation or dissipation properties of original systems.
- They are unconditionally stable and suitable for long time computation.

C. The literature review and the current work

In recent years, different numerical techniques are developed for the solution of Eq.(1), such as, Hu [20] proposed a multi-symplectic method for the KdV-mKdV equation. Wang [21] developed a multi-symplectic Fourier pseudo-spectral scheme for the Gardner equation. Nishiyama [22] proposed two energy-preserving finite difference schemes for the Gardner equation. However, there are few results about structure-preserving methods for the Gardner equation. Yan [23] proposed a class of nonlinear conservative schemes for the complex KdV equation. However, most of the proposed schemes are nonlinear and need an iterative solver. Thus, in this paper, we will develop a class of linear implicit energy-preserving scheme and a class of linear explicit momentum-preserving scheme, which are accurate and unconditionally stable (with long time computation ability) for the Gardner equation. The proposed schemes only need to solve a linear system at each time step and the schemes not require to solve the inverse of the matrix corresponding to the linear system. Thus, the proposed schemes are efficient with respect to the nonlinear schemes.

The organization of this paper is as follows. In Section 2, the proposed schemes are derived and their conservation properties are analyzed. In Section 3, the linear stability of the proposed schemes are analyzed. Section 4 gives some numerical examples to illustrate the efficiency of the proposed schemes. A simple conclusion is provided in Section 5.

II. Numerical schemes

In this section, we derived the proposed schemes and analyzed their conservation properties.

In what follows, the numerical solution at (x_k, t_m) is denoted by $U_k^{(m)}$, and the following periodic boundary conditions

$$\frac{\partial^j u}{\partial x^j}\Big|_{x=a} = \frac{\partial^j u}{\partial x^j}\Big|_{x=b} (j = 0, 1, 2).$$

are specified for the Gardner equation. In addition, we define the inner product of two functions, $u(x)$ and $v(x)$, as $(u(x), v(x)) \equiv \int_a^b u(x)v(x)\,dx$.

A. The proposed schemes

In order to derive the proposed schemes, we will adopt the concept of variational derivatives. See also the monograph [8]. we first define "free energy" or "local energy" of the Gardner equation (1) as:

$$G(u, u_x) = \frac{\alpha}{3}u^3 - \frac{\beta}{4}u^4 - \frac{\mu}{2}\left(\frac{\partial u}{\partial x}\right)^2, \tag{2}$$

and integrate the "local energy" over the solution domain to obtain the "global energy", $J(u) = \int_a^b G(u, u_x)\,dx$.

Then Eq. (1) can be written as

$$u_t = -\frac{\partial}{\partial x}\left(\frac{\delta G}{\delta u}\right), \tag{3}$$

where $\delta G/\delta u = \alpha u^2 - \beta u^3 + \mu u_{xx}$ is the variational derivative of $G(u, u_x)$ defined by $\frac{\delta G}{\delta u} = \frac{\partial G}{\partial u} - \frac{\partial}{\partial x}\left(\frac{\partial G}{\partial u_x}\right)$.

We first define a linear scheme of "local energy" (2) as

$$\begin{aligned} G_{d,k}(U^{(m+1)}, U^{(m)}) &= \frac{\alpha}{6}\left[U_k^{(m+1)}(U_k^{(m)})^2 + U_k^{(m)}(U_k^{(m+1)})^2\right] \\ &- \frac{\beta}{4}(U_k^{(m)})^2(U_k^{(m+1)})^2 - \frac{\mu}{8}\left[(\delta_k^+ U_k^{(m+1)})^2 + (\delta_k^- U_k^{(m+1)})^2\right. \\ &\left.+ (\delta_k^+ U_k^{(m)})^2 + (\delta_k^- U_k^{(m)})^2\right], \end{aligned} \tag{4}$$

where $\delta_k^+ U_k^{(m)} = (U_{k+1}^{(m)} - U_k^{(m)})/h, \quad \delta_k^- U_k^{(m)} = (U_k^{(m)} - U_{k-1}^{(m)})/h.$

Then we obtain a linear scheme of $\delta G/\delta u$,

$$\begin{aligned} \frac{\delta G_d}{\delta(U^{(m+1)}, U^{(m)}, U^{(m-1)})_k} &= \frac{\alpha}{3}U_k^{(m)}(U_k^{(m-1)} + U_k^{(m)} \\ &+ U_k^{(m+1)}) - \frac{\beta}{2}(U_k^{(m)})^2(U_k^{(m+1)} + U_k^{(m-1)}) \\ &+ \frac{\mu}{2}\delta_k^{\langle 2\rangle}(U_k^{(m)} + U_k^{(m+1)}), \end{aligned} \tag{5}$$

where $\sum_{k=0}^{N}{}'' f_k \triangleq \frac{1}{2}f_0 + f_1 + \cdots + f_{N-1} + \frac{1}{2}f_N$ denotes a trapezoidal rule.

In the following, we will derive the proposed schemes by resorting to the FVEM [11].

We multiply both sides of the Eq.(3) by each one of the test functions ψ_i, i=1, 2,..., N, and integrate the product over the solution domain to obtain the following semi-discrete scheme:

$$(\delta_m^{\langle 1\rangle} U^{(m)}, \psi_i) = -\left(\left(\frac{\delta G_d}{\delta(U^{(m+1)}, U^{(m)}, U^{(m-1)})}\right)_x, \psi_i\right), \tag{6}$$

i=1, 2,..., N, and $\delta_m^{\langle 1\rangle} U^{(m)} = (U^{(m+1)} - U^{(m-1)})/2\Delta t$.

Substituting (5) into (6), we obtain its fully-discrete scheme. The above method is a linear scheme and can precisely conserve the mass and energy of the original system. Thus, the above method is named the linear energy-preserving finite volume element method (LEFVEM).

At the same time, Eq. (1) also conserve the momentum K, thus we hope that the numerical methods still retain this property. To this end, like the forward process, we first define a scheme of "local energy" as follows:

$$\begin{aligned} G_{d,k}(U^{(m)}) &= \frac{\alpha}{3}(U_k^{(m)})^3 - \frac{\beta}{4}(U_k^{(m)})^4 \\ &- \frac{\mu}{2}\left(\frac{(\delta_k^+ U_k^m)^2 + (\delta_k^- U_k^m)^2}{2}\right). \end{aligned} \tag{7}$$

Then, by resorting to (7) and the discrete variational derivative method, we obtain another scheme of the variational derivative $\delta G/\delta u$:

$$\begin{aligned} \frac{\delta G_d}{\delta(U^{(m+1)}, U^{(m)})_k} &= \frac{\alpha}{3}[(U_k^{(m+1)})^2 + U_k^{(m+1)}U_k^{(m)} \\ &+ (U_k^{(m)})^2] - \frac{\beta}{4}[(U_k^{(m+1)})^2 + (U_k^{(m)})^2](U_k^{(m+1)} + U_k^{(m)}) \\ &+ \frac{\mu}{2}\delta_k^{\langle 2\rangle}(U_k^{(m)} + U_k^{(m+1)}). \end{aligned} \tag{8}$$

Let $(U_+^{(m)})_k = U_{k+1}^{(m)}$ and $(U_-^{(m)})_k = U_{k-1}^{(m)}$, and substitute them into (8) and in place of $U_k^{(m+1)}$ and $U_k^{(m)}$, respectively. Then we obtain a new scheme of variational derivative $\delta G/\delta u$:

$$\frac{\delta G_d}{\delta(U_+^{(m)}, U_-^{(m)})_k} = \frac{\alpha}{3}[(U_{k+1}^{(m)})^2 + U_{k+1}^{(m)}U_{k-1}^{(m)} + (U_{k-1}^{(m)})^2] - \frac{\beta}{4}[(U_{k+1}^{(m)})^2 + (U_{k-1}^{(m)})^2](U_{k+1}^{(m)} + U_{k-1}^{(m)}) + \frac{\mu}{2}\delta_k^{\langle 2\rangle}(U_{k+1}^{(m)} + U_{k-1}^{(m)}). \tag{9}$$

We multiply both sides of (3) by each one of the test functions ψ_j, j=1, 2, ..., N, and integrate the product over the solution domain to obtain the following semi-discrete scheme:

$$(\delta_m^{\langle 1\rangle}U^{(m)}, \psi_j) = -\left(\frac{\partial}{\partial x}\left(\frac{\delta G_d}{\delta(U_+^{(m)}, U_-^{(m)})}\right), \psi_j\right), \tag{10}$$

j=1, 2,..., N.

Substituting (9) into (10), we obtain the corresponding fully-discrete scheme of (10). The above method is a linear scheme and can precisely conserve the mass and momentum of the original system. Thus, the above method is called the linear momentum-preserving finite volume element method (LMFVEM).

In addition, for comparison, we also propose a Crank-Nicolson finite volume element method (CNFVEM) [24] and a Runge-Kutta [25] finite volume element method (RK-FVEM) for the Gardner equation (1).

The semi-discrete CNFVEM is presented as follows:

$$\begin{aligned}&(\delta_m^{\langle 1\rangle}U^{(m+1/2)}, \psi_k) = \beta(F_1(U)_x^{(m+1/2)}, \psi_k)\\ &- \alpha((F_2(U)^{(m+1/2)} - \mu U_{xx}^{(m+1/2)})_x, \psi_k),\end{aligned} \tag{11}$$

where k=1, 2,..., N, and

$$\delta_m^{\langle 1\rangle}U^{(m+1/2)} = \frac{U^{(m+1)} - U^{(m)}}{\Delta t},$$
$$F_1(U)^{(m+1/2)} = \frac{(U^{(m)})^3 + (U^{m+1})^3}{2},$$
$$F_2(U)^{(m+1/2)} = \frac{(U^{(m)})^2 + (U^{(m+1)})^2}{2}.$$

Similarly, the RKFVEM is derived as follows:

$$(u_t, \psi_k) = \big((\beta F_1(u) - \alpha F_2(u) - \mu u_{xx})_x, \psi_k\big), \tag{12}$$

where k=1, 2, ..., N, $F_1(u) = u^3$, $F_2(u) = u^2$, and the third order Heun Runge-Kutta method is used for the time discretization.

In this paper, we mainly concerned with the conservation of the first integrals of the proposed schemes. The discrete mass, momentum, and energy are respectively defined as

$$\begin{aligned}M_d &= \frac{1}{2}\sum_{k=0}^{N}{}''(U_k^{(m)} + U_k^{(m+1)})\Delta x,\\ K_d &= \frac{1}{2}\sum_{k=0}^{N}{}''U_k^{(m)}U_k^{(m+1)}\Delta x,\\ J_d &= \sum_{k=0}^{N}{}''G_{d,k}(U_k^{(m)}, U_k^{(m+1)})\Delta x,\end{aligned} \tag{13}$$

where $G_{d,k}(U_k^{(m)}, U_k^{(m+1)})$ is defined by (4).

Remark II.1. *The LEFVEM is a three-level linear energy-preserving scheme. The initial value $U^{(1)}$ is approximated by the the following energy-preserving method [11]*

$$\left(\frac{U^{(1)} - U^{(0)}}{\Delta t}, \psi_i\right) = -\left(\frac{\partial}{\partial x}\left(\frac{\delta G_d}{\delta(U^{(1)}, U^{(0)})}\right), \psi_i\right), \tag{14}$$

where i=1, 2,..., N, and

$$\frac{\delta G_d}{\delta(U^{(1)}, U^{(0)})_k} = \frac{\alpha}{3}[(U_k^{(1)})^2 + U_k^{(1)}U_k^{(0)} + (U_k^{(0)})^2] - \frac{\beta}{4}[(U_k^{(1)})^2 + (U_k^{(0)})^2](U_k^{(1)} + U_k^{(0)}) + \frac{\mu}{2}\delta_k^{\langle 2\rangle}(U_k^{(0)} + U_k^{(1)}).$$

Remark II.2. *The LMFVEM is a three-level linear momentum-preserving scheme. The initial value $U^{(1)}$ is approximated by the the following momentum-preserving method [11]*

$$\left(\frac{U^{(1)} - U^{(0)}}{\Delta t}, \psi_i\right) = -\left(\frac{\partial}{\partial x}\left(\frac{\delta G_d}{\delta(U_+^{(0)}, U_-^{(0)})}\right), \psi_i\right), \tag{15}$$

where i=1, 2,..., N, and

$$\begin{aligned}\frac{\delta G_d}{\delta(U_+^{(0)}, U_-^{(0)})_k} &= \frac{\alpha}{12}\big[(U_{k+1}^{(1)} + U_{k+1}^{(0)})^2\\ &+ (U_{k+1}^{(1)} + U_{k+1}^{(0)})(U_{k-1}^{(1)} + U_{k-1}^{(0)}) + (U_{k-1}^{(1)} + U_{k-1}^{(0)})^2\big]\\ &- \frac{\beta}{32}\big[(U_{k+1}^{(1)} + U_{k+1}^{(0)})^2 + (U_{k-1}^{(1)} + U_{k-1}^{(0)})^2\big]\\ &(U_{k+1}^{(1)} + U_{k+1}^{(0)} + U_{k-1}^{(1)} + U_{k-1}^{(0)}) + \frac{\mu}{4}\delta_k^{\langle 2\rangle}(U_{k+1}^{(1)} + U_{k+1}^{(0)}\\ &+ U_{k-1}^{(1)} + U_{k-1}^{(0)}).\end{aligned}$$

B. Conservation properties of the schemes

In this section, we study the conservation properties of the LEFVEM and the LMFVEM.

We first study the conservation properties of the LEFVEM, which can precisely conserve the discrete mass and energy.

Theorem II.1. *(Mass conservation law) Let $U = U^{(m)}$ be the solution of (6), and suppose the following conditions are satisfied, namely*

$$\Big[-\frac{\delta G_d}{\delta(U^{(m+1)}, U^{(m)}, U^{(m-1)})}\Big]_{x=a}^{b} = 0,$$

then the solution of the scheme (6) satisfies

$$\frac{1}{2}\int_a^b (U^{(m)} + U^{(m+1)})\,dx = const.$$

The conservation of mass can be easily proved, which is similar as [23].

Theorem II.2. *(Energy conservation law) Let $U = U^{(m)}$ be the solution of (6), and suppose the following conditions are satisfied, namely*

$$\Big[-\frac{1}{2}\Big(\frac{\delta G_d}{\delta(U^{(m+1)}, U^{(m)}, U^{(m-1)})}\Big)^2\Big]_{x=a}^{b} = 0,$$

then the solution of the scheme (6) satisfies

$$\int_a^b G_d(U^{(m+1)}, U^{(m)})\,dx = const,$$

where $G_d(U^{(m+1)}, U^{(m)})$ is defined by (4).

Proof:

$$\frac{1}{2\Delta t}\int_a^b \left(G_d(U^{(m+1)}, U^{(m)}) - G_d(U^{(m)}, U^{(m-1)})\right) dx$$
$$= \int_a^b \frac{\delta G_d}{\delta(U^{(m+1)}, U^{(m)}, U^{(m-1)})}\left(\frac{U^{(m+1)} - U^{(m-1)}}{2\Delta t}\right) dx$$
$$= -\frac{1}{2}\int_a^b \frac{\partial}{\partial x}\left(\frac{\delta G_d}{\delta(U^{(m+1)}, U^{(m)}, U^{(m-1)})}\right)^2 dx$$
$$= \left[-\frac{1}{2}\left(\frac{\delta G_d}{\delta(U^{(m+1)}, U^{(m)}, U^{(m-1)})}\right)^2\right]_{x=a}^b = 0.$$

■

Next, we study the conservation properties of the LMFVEM, which can precisely conserve the discrete mass and momentum.

Theorem II.3. *(Mass conservation law) Let $U = U^{(m)}$ be the solution of (10), and assume the following conditions are satisfied, namely*

$$\left[-\frac{\delta G_d}{\delta(U_+^{(m)}, U_-^{(m)})}\right]_{x=a}^b = 0,$$

then the solution of the scheme (10) satisfies

$$\frac{1}{2}\int_a^b (U^{(m)} + U^{(m+1)})\, dx = const.$$

Theorem II.4. *(Momentum conservation law) Let $U = U^{(m)}$ be the solution of (10), and assume the following conditions are satisfied, namely*

$$-\left[U^{(m)}\frac{\delta G_d}{\delta(U_+^{(m)}, U_-^{(m)})}\right]_{x=a}^b, \quad \left[G_d(U^{(m)})\right]_{x=a}^b = 0,$$

then the solution of the scheme (10) satisfies

$$\frac{1}{2}\int_a^b U^{(m)}U^{(m+1)}\, dx = const.$$

Proof:

$$\frac{1}{2\Delta t}\left[K_d(U^{(m+1)}, U^{(m)}) - K_d(U^{(m)}, U^{(m-1)})\right]$$
$$= \int_a^b U^{(m)}\delta_m^{\langle 1\rangle}U^{(m)}\, dx$$
$$= -\int_a^b U^{(m)}\frac{\partial}{\partial x}\left(\frac{\delta G_d}{\delta(U_+^{(m)}, U_-^{(m)})}\right) dx$$
$$= \int_a^b \frac{\partial U^{(m)}}{\partial x}\frac{\delta G_d}{\delta(U_+^{(m)}, U_-^{(m)})}\, dx$$
$$= \int_a^b \frac{\partial G_d}{\partial x}\, dx = 0.$$

■

At last, the scheme (11) conserve the discrete global mass.

Theorem II.5. *(Mass conservation law) Let $U = U^{(m)}$ be the solution of (11), and suppose the following conditions are satisfied, namely*

$$-\left[\beta F_1(U)^{(m+1/2)} - \alpha F_2(U)^{(m+1/2)} - \mu U_{xx}^{(m+1/2)}\right]_{x=a}^b = 0,$$

then the solution of the scheme (11) satisfies

$$\int_a^b U^{(m)}\, dx = const.$$

III. Linear stability analysis

In this section, we analyze the linear stability of the the LEFVEM and the LMFVEM using the technique of Von Neumann approach. The LEFVEM and the LMFVEM are unconditionally linear stable under periodic boundary condition.

Theorem III.1. *Let $U = U^{(m)}$ be the solution of (6) and (10), and assume it satisfy the periodic boundary condition, then the LEFVEM and the LMFVEM are unconditionally linear stable.*

Proof: First of all, we consider the LEFVEM (6), which can be written as the following form:

$$\begin{aligned}
&-\alpha_1 U_{k-2}^{(m+1)} + \alpha_2 U_{k-1}^{(m+1)} + \alpha_3 U_k^{(m+1)} - \alpha_2 U_{k+1}^{(m+1)} \\
&+ \alpha_1 U_{k+2}^{(m+1)} = \alpha_1 U_{k-2}^{(m-1)} - \alpha_2 U_{k-1}^{(m-1)} + \alpha_3 U_k^{(m-1)} \\
&+ \alpha_2 U_{k+1}^{(m-1)} - \alpha_1 U_{k+2}^{(m-1)} + \alpha_4\big[U_{k-1}^{(m)}(U_{k-1}^{(m-1)} + U_{k-1}^{(m)} \\
&+ U_{k-1}^{(m+1)}) - U_{k+1}^{(m)}(U_{k+1}^{(m-1)} + U_{k+1}^{(m)} + U_{k+1}^{(m+1)})\big] \\
&+ \alpha_5\big[(U_{k+1}^{(m)})^2(U_{k+1}^{(m+1)} + U_{k+1}^{(m-1)}) \\
&- (U_{k-1}^{(m)})^2(U_{k-1}^{(m+1)} + U_{k-1}^{(m-1)})\big], k = 0, 1, \ldots, N,
\end{aligned}$$

where $\alpha_1 = 3\mu\Delta t$, $\alpha_2 = 6\mu\Delta t$, $\alpha_3 = 6h^3$, $\alpha_4 = 2\alpha h^2\Delta t$, and $\alpha_5 = 3\beta h^2\Delta t$. For the stability analysis, we consider the linear version of the above scheme, and let $C = \max_{0\le k\le N}\{|U_k^{(m)}|\}$, then we have

$$\begin{aligned}
&-\alpha_1 U_{k-2}^{(m+1)} + \alpha_2 U_{k-1}^{(m+1)} + \alpha_3 U_k^{(m+1)} - \alpha_2 U_{k+1}^{(m+1)} \\
&+ \alpha_1 U_{k+2}^{(m+1)} = \alpha_1 U_{k-2}^{(m-1)} - \alpha_2 U_{k-1}^{(m-1)} + \alpha_3 U_k^{(m-1)} \\
&+ \alpha_2 U_{k+1}^{(m-1)} - \alpha_1 U_{k+2}^{(m-1)} + C\alpha_4\big(U_{k-1}^{(m-1)} + U_{k-1}^{(m)} \\
&+ U_{k-1}^{(m+1)} - U_{k+1}^{(m-1)} - U_{k+1}^{(m)} - U_{k+1}^{(m+1)}\big) \\
&+ C^2\alpha_5\big(U_{k+1}^{(m+1)} + U_{k+1}^{(m-1)} - U_{k-1}^{(m+1)} - U_{k-1}^{(m-1)}\big),
\end{aligned}$$

To apply Von Neumann method, we set $U_k^{(m)} = V^m(\xi)e^{i\xi kh}$ and substitute it into the above linearized schemes and cancel the common factor of $e^{i\xi kh}$ gives the following relation for $V \equiv V(\xi)$:

$$(\alpha_3 + i\beta)V^{m+1}(\xi) - (\alpha_3 - i\beta)V^{m-1}(\xi) + 2\gamma V^m(\xi) = 0,$$

where $\beta = 2(\alpha_1\sin(2\xi h) - \alpha_2\sin(\xi h) + C\alpha_4\sin(\xi h) - C^2\alpha_5\sin(\xi h))$, $\gamma = iC\alpha_4\sin(\xi h)$.

Let $V^m(\xi) = g^m$, and divide by $(\alpha_3 - i\beta)g^{m-1}$, we obtain a quadratic equation for g,

$$(\alpha_3 + i\beta)g^2 + 2\gamma g - (\alpha_3 - i\beta) = 0.$$

Then we can obtain its eigenvalues by solving the above quadratic equation

$$g_{1,2} = \frac{-\gamma \pm \sqrt{(\alpha_3^2 + \beta^2) + \gamma^2}}{\alpha_3 + i\beta}.$$

After a series of straightforward computation, we obtain $|g_1|^2 = 1$ and $|g_2|^2 = 1$. Thus, the LEFVEM (6) is unconditionally linear stable. ■

Similarly, we can also prove that the LMFVEM (10) is also unconditionally linear stable.

IV. Numerical experiments

In this section, we present several numerical examples to illustrate the efficiency of the proposed schemes. In particular, we analyze the numerical errors and the conservation properties of the proposed schemes, and compare them with the CNFVEM and the RKFVEM. All computational results are obtained in Matlab software R2009 on a computer with 3.2 GHz CPU and 8 GB RAM.

A. Single solitary wave

In this example, we consider the following Gardner equation

$$u_t + 6uu_x - 6u^2u_x + u_{xxx} = 0, -40 \le x \le 40, t > 0, \quad (16)$$

which subject to the periodic boundary condition $u(-40, t) = u(40, t)$. The above equation has the following exact solution

$$u(x,t) = \frac{\kappa^2}{1 + \sqrt{1-\kappa^2}\cosh[\kappa(x - \kappa^2 t - x_0)]},$$

where $\kappa \in (0, 1)$ and x_0 is a given constant.

In this example, unless otherwise specified, the wave is initially centered at $x_0 = 15$ and $\kappa = 0.8$. This solution represents a solitary wave with an amplitude that ranges from zero to one, and initially located at $x = x_0$. For convenience, the initial values $U^{(0)}$ and $U^{(1)}$ of the three-level schemes (6) and (10) are respectively approximated by $u(x, 0)$ and $u(x, 1)$.

In order to estimate the numerical errors and the convergence rates of the proposed schemes in both the spatial and temporal variables, we consider the normalized L_2-norm defined by $E(t) = \|U^n - u(\cdot, t)\|/\|u(\cdot, t)\|$, $t = n\Delta t$, n=1, 2, $\dots$.

In order to measure the spatial errors and the rates of convergence of the proposed methods, space steps $h = 1/2, 1/4, 1/8, 1/16$, and a small time step $\Delta t = 0.0001$ are taken to render the temporal errors negligible. The L_2 errors were recorded at $t = 0.1, 0.5$ and 1, respectively. The convergence rate corresponding to different runs with different spatial meshes $2h$ and h is defined to be $\log_2 (E_{2h}/E_h)$, as usual. The convergence rates and the associated spatial errors are presented in Tables I and II. From the results, we clearly see that the convergence rates of the LEFVEM and the LMFVEM are 2. Moreover, the LEFVEM is more accurate than the LMFVEM. Similarly, in order to estimate the temporal errors of the LEFVEM, a small space step $h = 1/32$ is adopted to render the spatial errors negligible, and the time steps $\Delta t = 1/2, 1/4, 1/8, 1/16$ are chosen for the LEFVEM. The L_2 errors were recorded at $t = 1, 2$ and 3, respectively. Table III presents the temporal accuracy and the convergence rates. It can be observed that the convergence rate of the LEFVEM is also 2.

For the LMFVEM, in fact, it is a explicit scheme, thus it is hard to see the asymptotic rate of the temporal error. Thus, as in [26], we made a reference calculation for a fixed value of h. We took a small value $\Delta t = \Delta t_{ref} = h/5000$, then the approximate solution $U^{(m)} = U^{(m)}(h, \Delta t_{ref})$ obtained by the reference simulation differs from the exact solution by an error that is almost purely from the spatial direction. For the same values of h, we then define a modified error as $E^*(t) = \|U^{(n)}(h, \Delta t) - U^{(m)}(h, \Delta t_{ref})\|/\|u(\cdot, t)\|$, where $t = n\Delta t = m\Delta t_{ref}$, and the values of Δt are larger than Δt_{ref}. The modified temporal errors and corresponding convergence rates are presented in Table IV, which clearly shows that the convergence rate of the LMFVEM is also 2 in time direction. Besides, for comparison, we also present the errors evaluated by the L_2 norm.

In order to further illustrate the accuracy of the proposed schemes, we compare the abstract errors of the numerical solution at $t = 5, 10$ and 20 for four different methods in Figs.2. In these figures, one can see that the LMFVEM has largest errors and the other proposed schemes have nearly the same errors. Besides, we also compare the conservative properties of the proposed schemes. To this end, we define the relative errors of the invariants as $\log(|I^{(n)} - I^{(0)}|/|I^{(0)}|)$. $I^{(n)}$ denotes the global invariants (13) evaluated along the numerical solution, and $I^{(0)}$ denotes the global invariants evaluated along the initial solution. In Fig.3, we compare the relative errors in the energy and momentum for four different methods, LEFVEM, LMFVEM, CNFVEM (which are all second order), and a third order RKFVEM. We choose third order RKFVEM because it has higher order accuracy than the other methods, but it does not exactly preserve the conservative properties of the governing equations, giving a clear demonstration of the practical advantages of a structure-preserving algorithms. Fig.3 shows that the LEFVEM can precisely conserve the energy at the discrete level, and the LMFVEM can precisely conserve the discrete momentum. This is an important result for the proposed methods which are all second-order, but demonstrate clear advantages over the higher-order method that is not structure-preserving. Thus, we conclude that the order of truncation error should not be the only deciding factor on which method is used in practice, and the structure-preservation is also an important factor.

In what follows, we will test the conservative properties of the proposed methods for a long time computation. To this end, we will consider the Gardner equation (16) over the interval $[-40, 40]$, subject to the aforementioned periodic boundary conditions.

The exact solution is taken as

$$u(x,t) = \begin{cases} \frac{\kappa^2}{1+\sqrt{1-\kappa^2}\cosh[\kappa(x-t_0)]}, x \in [-40 + t_0, 40], \\ \frac{\kappa^2}{1+\sqrt{1-\kappa^2}\cosh[\kappa(x-t_0+80)]}, x \in [-40, -40 + t_0), \end{cases}$$

where $t_0 = mod(t, 80)$.

The above solution represents a solitary wave and it will travel to initial position after a period of 80. We perform a simulation with space step $h = 1/5$ and time step $\Delta t = 0.01$ for a single solitary wave over $[-40, 40]$, and the computations is done up to time $t = 1000$. Fig.4 presents the numerical solutions of the LEFVEM in the time interval $[0, 20]$ and $[900, 1000]$, respectively. In Fig.4a one can see that the solitary wave initially located at $x_0 = 0$, and the wave moves to the right at a constant speed and the amplitude almost unchanged as time processes, as is expected. In addition, the relative errors of the proposed methods are presented in Fig. 5, which is in agreement with the theory results.

TABLE I: Errors $E(t)$ and spatial rates of convergence for the LEFVEM with $\Delta t = 0.0001$, $\kappa = 0.8$ and $x_0 = 15$.

h	$t = 0.1$		$t = 0.5$		$t = 1$	
	$E(t)$	order	$E(t)$	order	$E(t)$	order
1/2	$2.2148e-04$	—	$1.1000e-03$	—	$2.3000e-03$	—
1/4	$5.5806e-05$	1.99	$2.9216e-04$	1.91	$5.9143e-04$	1.96
1/8	$1.4087e-05$	1.99	$7.3713e-05$	1.99	$1.4892e-04$	1.99
1/16	$3.5324e-06$	2.00	$1.8471e-05$	2.00	$3.7293e-05$	2.00

TABLE II: Errors $E(t)$ and spatial rates of convergence for the LMFVEM with $\Delta t = 0.0001$, $\kappa = 0.8$ and $x_0 = 15$.

h	$t = 0.1$		$t = 0.5$		$t = 1$	
	$E(t)$	order	$E(t)$	order	$E(t)$	order
1/2	$1.1000e-03$	—	$5.7000e-03$	—	$1.1300e-02$	—
1/4	$2.9106e-04$	1.92	$1.4000e-03$	2.03	$2.9000e-03$	1.96
1/8	$7.3026e-05$	1.99	$3.6191e-04$	1.95	$7.2841e-04$	1.99
1/16	$1.8276e-05$	2.00	$9.0775e-05$	2.00	$1.8257e-04$	2.00

TABLE III: Errors $E(t)$ and temporal rates of convergence for the LEFVEM with $h = 1/32$, $\kappa = 0.8$ and $x_0 = 15$.

Δt	$t = 1$		$t = 2$		$t = 3$	
	$E(t)$	order	$E(t)$	order	$E(t)$	order
1/2	$5.8000e-03$	—	$9.7000e-03$	—	$1.3800e-02$	—
1/4	$1.4000e-03$	2.05	$2.6000e-03$	1.90	$3.6000e-03$	1.94
1/8	$3.8296e-04$	1.87	$6.9227e-04$	1.91	$9.3179e-04$	1.95
1/16	$9.9644e-05$	1.94	$1.7851e-04$	1.96	$2.3834e-04$	1.97

TABLE IV: Errors $E(t)$ and temporal rates of convergence for the LEFVEM with $h = 1/16$, $\Delta t_{ref} = \frac{1}{5000}h$, $t = 0.01$ and $x_0 = 15$.

Δt	$\Delta t h^{-1}$	$E(T)$	$E^*(T)$	order
1/10000	1/625	$1.8365e-06$	$1.0501e-09$	—
1/20000	1/1250	$1.8364e-06$	$6.0831e-10$	0.79
1/40000	1/2500	$1.8364e-06$	$1.5129e-10$	2.01
1/80000	1/5000	$1.8364e-06$	$3.5763e-011$	2.08
REF				
1/160000	1/10000	$1.8364e-06$		

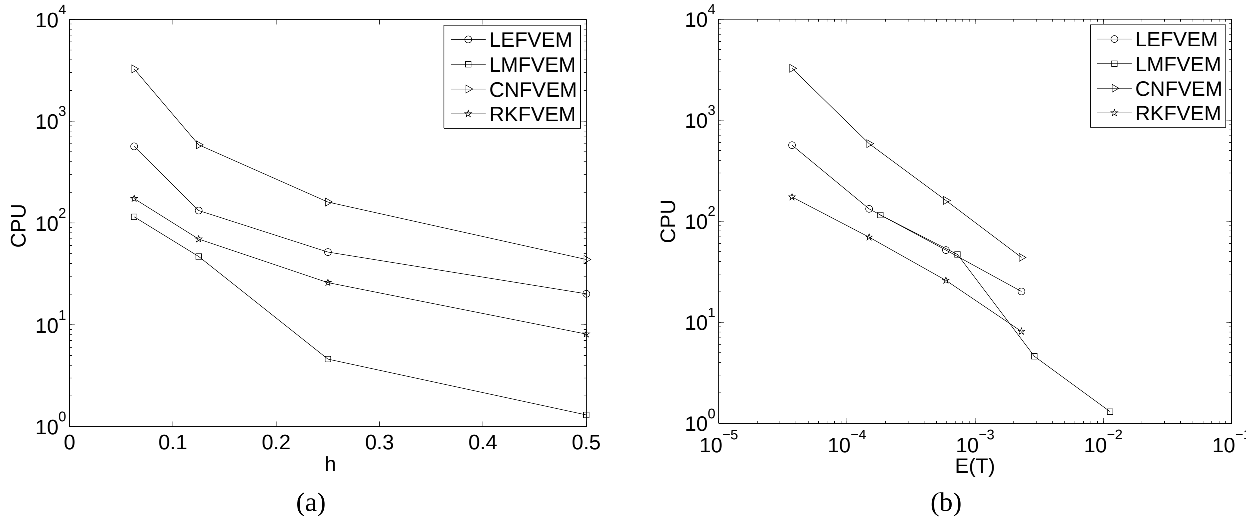

(a) (b)

Fig. 1: (a) CPU time of the proposed schemes, plotted against the spatial steps h,(b) CPU time versus error $E(T)$.

B. *Interaction of two solitary waves*

Now, we turn to consider the interaction of two solitary waves with different amplitudes. The initial solution is given as follows:

$$u(x,0) = \sum_{i=1}^{2} \frac{\kappa_i^2}{1 + \sqrt{1-\kappa_i^2}\cosh[\kappa_i(x - x_i)]}, \tag{17}$$

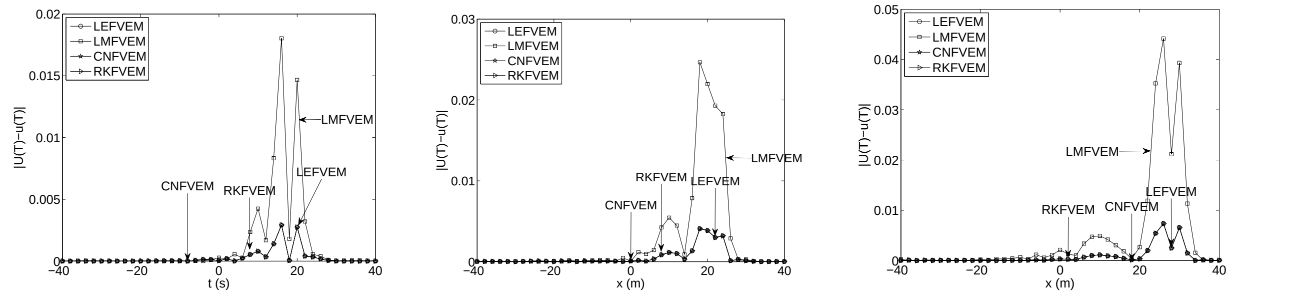

(a) (b) (c)

Fig. 2: Abstract errors of the numerical solutions obtained by the proposed schemes with $h = 1/8$, $\Delta t = 0.001$, (a) T=5, (b) T=10, (c) T=20.

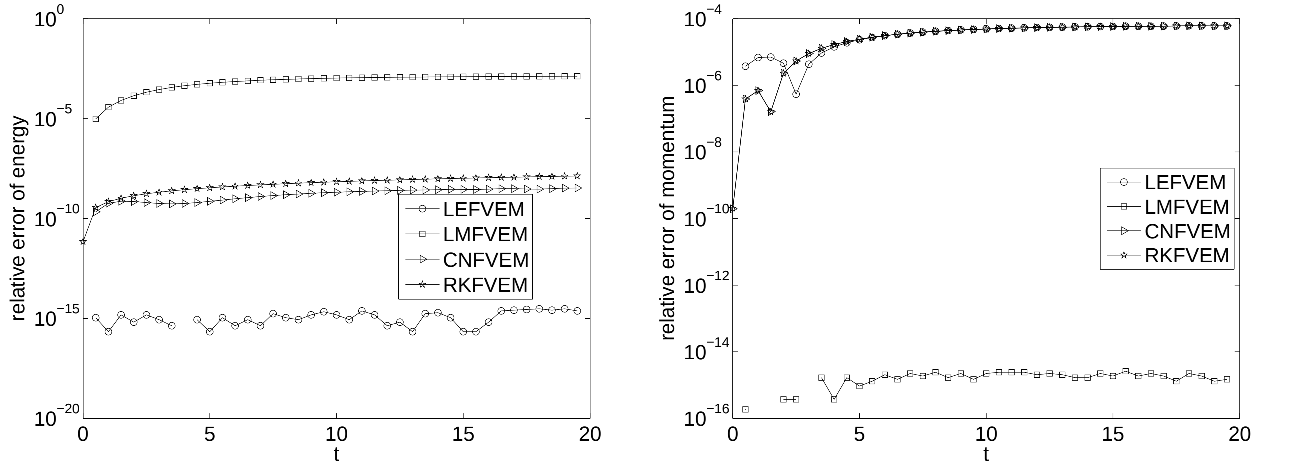

(a) (b)

Fig. 3: (a) relative error of the energy for different methods with $h = 1/8$, $\Delta t = 0.001$ and $T = 20$, (b) relative error of the momentum.

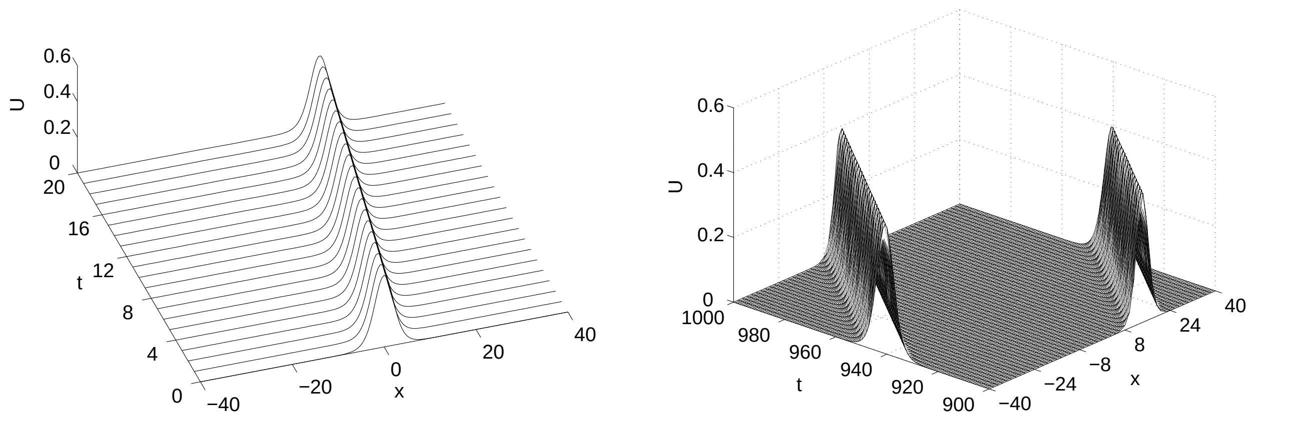

(a) (b)

Fig. 4: Numerical solutions of the LEFVEM with $h = 1/5$, $\Delta t = 0.01$, $\kappa = 0.8$ and $x_0 = 0$: (a) $t \in [0, 20]$, (b)$t \in [900, 1000]$.

where $\kappa_i \in (0, 1)$ and x_i, (i=1, 2) are arbitrary constants. This solution represents two solitary waves with different amplitudes, one initially located at x_1 and the other located at x_2, and moving towards the same direction. The problem is considered in the interval $[-40, 40]$, and the corresponding parameters are chosen as $\kappa_1 = 0.9$, $\kappa_2 = 0.6$, $x_1 = -5$ and $x_2 = 15$. Here, the initial value $U^{(1)}$ at the second level is respectively approximated by the scheme (14) and the scheme (15) for the LEFVEM and the LMFVEM.

Fig.6a presents the surface plot of the numerical solution of the LEFVEM. Fig.6b shows the interaction process of two solitary wave at different times. It is clearly seen that the taller wave initially located at the left of the shorter wave, and at about $t = 27.5$, the taller wave catches up with the shorter wave and two waves overlapped together; At about $t = 38.5$, two waves start to leave away, and at $t = 49.5$, two waves completely separate and continue to travel to the right. Fig.7 presents the relative errors of the invariants of

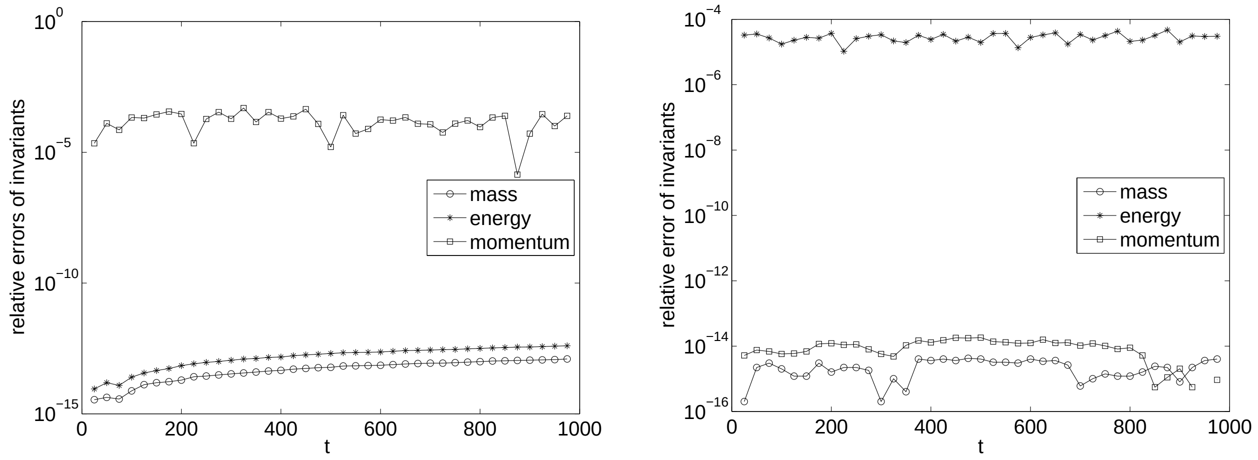

(a) (b)

Fig. 5: The relative errors of the invariants evaluated along the numerical solutions with $h = 1/5$, $\Delta t = 0.01$ and $t \in [0, 1000]$: (a) LEFVEM, (b) LMFVEM.

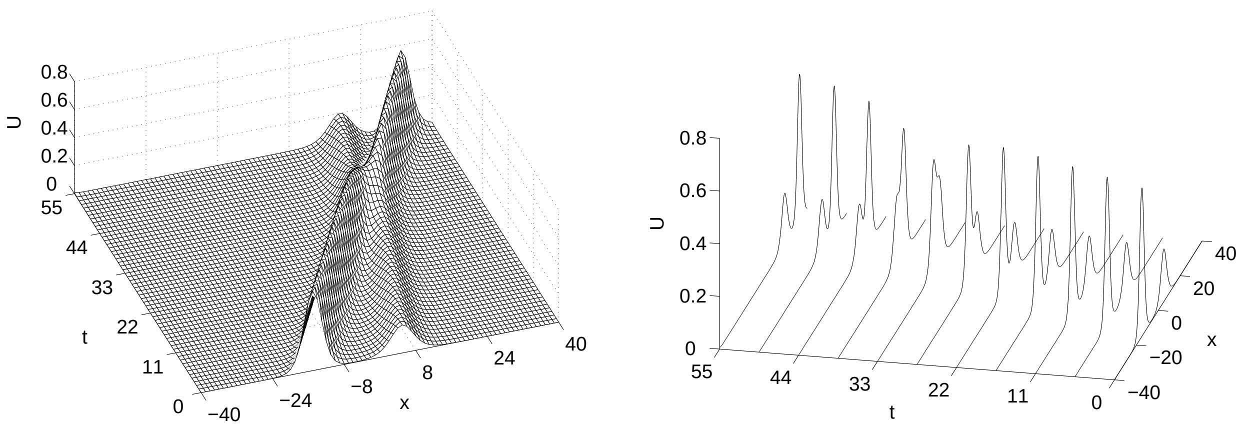

(a) (b)

Fig. 6: Numerical solution of the LEFVEM with $x_1 = -5$, $x_2 = 15$, $\kappa_1 = 0.9$, $\kappa_2 = 0.6$, $h = 1/4$ and $\Delta t = 0.1$: (a) surface plot, (b) the interaction process.

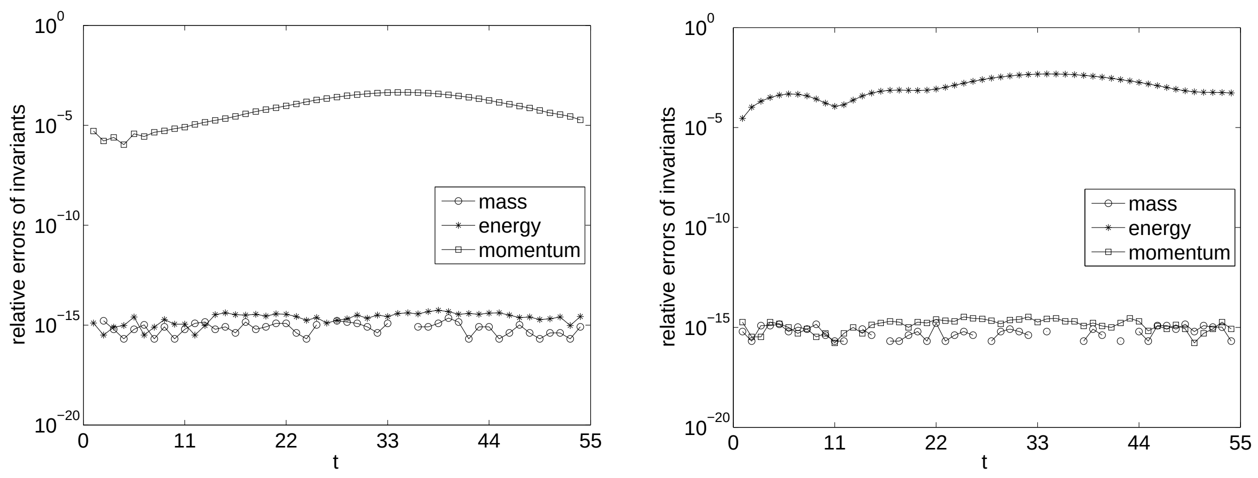

(a) (b)

Fig. 7: The relative errors of the invariants of the proposed methods: (a) LEFVEM with $h = 1/4$ and $\Delta t = 0.1$, (b) LMFVEM with $h = 1/4$, $\Delta t = 0.001$.

the proposed methods. It is noted that the LMFVEM need smaller time steps than the LEFVEM.

C. Zabusky-Kruskal wave

In order to further illustrate the effectiveness of the proposed scheme, we consider the the following Zabusky-

Kruskal's problem,

$$u_t + uu_x + (4.84 \times 10^{-4}) \times u_{xxx} = 0,$$

in the interval $[0, 2]$, subject to the periodic boundary condition $u(0,t) = u(2,t)$. The initial solution is given by $u(x, 0) = \cos(\pi x)$, and the initial value $U^{(1)}$ is also provided by the scheme (14) and (15).

As is stated in [27], the solution starts with a cosine wave and later develops a train of 8 solitary waves which travel at different speeds and interact with each other, detailed description about the solution, see [28]. According to [27], there are several critical moments for the solution:

- $t = t_c = \frac{1}{\pi} \approx 0.32$, the solution start to break up;
- $t = 3.6t_c \approx 1.15$, the solution develops into 8 solitary waves.

For computation, we set $h = 1/200$, $\Delta t = 0.01$ and the computations are done up to time $t = 10$. The numerical solution of the LEFVEM at $t = 0, 0.32, 1.15$ and $t = 10$ are presented in Fig.8a, which shows that, at $t = 0.32$, the solution start to break up; at $t = 1.15$, 8 solitary waves appears. The results are in well agreement with the numerical results obtained by Zabusky and Kruskal in 1965 [28]. The relative errors of the invariants corresponding to the LEFVEM are plotted in Fig.8b.

V. Conclusions

In this paper, the linear conservative finite volume element methods are proposed for the Gardner equation. The numerical results show that the linear LEFVEM and LMFVEM have better conservation properties than the CNFVEM and RKFVEM. Moreover, the proposed methods are more efficient than the classical nonlinear schemes. In addition, the LEFVEM is more stable than the LMFVEM, i.e. the LMFVEM needs smaller time steps.

References

[1] K. O. Abdulloev, B. I. L., and M. V. G., "One more example of inelastic solution interaction," *Physics Letters A*, vol. 56, no. 6, pp. 427–428, 1976.

[2] W. A. M., "New solitons and kinks solutions to the Sharma-Tasso-Olver equation," *Applied Mathematics and Computation*, vol. 188, no. 2, pp. 1205–1213, 2007.

[3] A. M. J. and S. H., *Solitons and the inverse scattering transform*. Philadelphia: SIAM, 1981.

[4] K. E. V., T. H., L. M., and B. A., "A study of shallow water waves with Gardner's equation," *Nonlinear Dynamics*, vol. 66, no. 4, pp. 497–507, 2011.

[5] V. V. M., D. P. A., H. M. Ts., and M. I. M., "Travelling wave solutions of the Gardner equation and motion of plane curves governed by the mKdV flow," *AIP Conference Proceedings*, vol. 1401, no. 1, pp. 86–93, 2011.

[6] M. Dahlby and O. Brynjulf, "A general framework for deriving integral preserving numerical methods for PDEs," *SIAM Journal on Scientific Computing*, vol. 35, no. 5, pp. 2318–2340, 2011.

[7] H. E., L. C., and W. G., *Geometric Numerical Integration: Structure-Preserving Algorithms for Ordinary Differential Equations*. Berlin: Springer-Verlag, 2006.

[8] D. Furihata and T. Matsuo, *Discrete variational derivative method: a structure-preserving numerical method for partial differential equations*. London: CRC Press, 2010.

[9] S. Koide and D. Furihata, "Nonlinear and linear conservative finite difference schemes for regularized long wave equation," *Japan Journal of Industrial and Applied Mathematics*, vol. 26, no. 1, pp. 15–40, 2009.

[10] T. Matsuo and D. Furihata, "Dissipative or conservative finite difference schemes for complex-valued nonlinear partial differential equations," *Journal of Computational Physics*, vol. 171, no. 2, pp. 425–447, 2001.

[11] J. L. Yan, Q. Zhang, and Z. Y. Zhang, "New conservative finite volume element schemes for the modified Korteweg-de Vries equation," *Mathematical Methods in the Applied Sciences*, vol. 39, no. 18, pp. 5149–5161, 2016.

[12] Y. Miyatake and T. Matsuo, "A general framework for finding energy dissipative/conservative H^1-Galerkin schemes and their underlying H^1-weak forms for nonlinear evolution equations," *BIT Numerical Mathematics*, vol. 54, no. 4, pp. 1119–1154, 2014.

[13] J. Yan and L. Zheng, "New energy-preserving finite volume element scheme for the Korteweg-de Vries equation," *IAENG International Journal of Applied Mathematics*, vol. 47, no. 2, pp. 223–232, 2017.

[14] Z. Q. Cai, "On the finite volume element method," *Numerische Mathematik*, vol. 58, pp. 713–735, 1991.

[15] Z. Y. Zhang and F. Q. Lu, "Quadratic finite volume element method for the improved Boussinesq equation," *Journal of Mathematical Physics*, vol. 53, no. 1, p. 013505, 2012.

[16] Q. X. Wang, Z. Y. Zhang, X. H. Zhang, and Q. Y. Zhu, "Energy-preserving finite volume element method for the improved Boussinesq equation," *Journal of Computational Physics*, vol. 270, pp. 58–69, 2014.

[17] R. E. Bank and D. J. Rose, "Some error estimates for the box methods," *SIAM Journal on Numerical Analysis*, vol. 24, no. 4, pp. 777–787, 1987.

[18] R. H. Li, Z. Y. Chen, and W. Wu, *Generalized Difference Methods for Differential Equations: Numerical Analysis of Finite Volume Methods*. New York: Marcel Dekker Inc., 2000.

[19] J. Yan and Z. Zhang, "Two-grid methods for characteristic finite volume element approximations of semi-linear Sobolev equations," *Engineering Letters*, vol. 23, no. 3, pp. 189–199, 2015.

[20] W. P. Hu, Z. C. Deng, Q. Y. Y., and Z. R. W., "Multi-symplectic method for the generalized $(2+1)$-dimensional KdV-mKdV equation," *Acta Mechanica Sinica*, no. 3, 2012.

[21] W. Z. H. and H. L. Y., "Multi-symplectic Fourier pseudo-spectral scheme for the combined KdV-mKdV equation," *Journal of Huaqiao University (Natural Science)*, no. 4, 2014.

[22] N. H. and N. T., "Conservative difference schemes for the numerical solution of the Gardner equation," *Computational and Applied Mathematics*, vol. 35, no. 1, pp. 75–95, 2016.

[23] Y. J.L. and Z. L.H., "Conservative finite volume element schemes for the complex modified Korteweg-de Vries equation," *International Journal of Applied Mathematics and Computer Science*, vol. 27, no. 3, pp. 515–525, 2017.

[24] Q. Feng, "Crank-nicolson difference scheme for a class of space fractional differential equations with high order spatial fractional derivative," *IAENG International Journal of Applied Mathematics*, vol. 48, no. 2, pp. 214–220, 2018.

[25] F. Wang and L. X.B, "A class of Lobatto methods of order 2s," *IAENG International Journal of Applied Mathematics*, vol. 46, no. 1, pp. 6–10, 2016.

[26] B. J. L., D. V. A., K. O. A., and M. W. R., "Conservative, high-order numerical schemes for the generalized Korteweg-de Vries equation," *Philosophical Transactions of the Royal Society. A: Mathematical, Physical and Engineering Sciences*, vol. 351, no. 1695, pp. 107–164, 1995.

[27] N. Y. Yi, Y. Q. Huang, and H. L. Liu, "A direct discontinuous Galerkin method for the generallized Korteweg-de Vries equation: Energy conservation and boundary effect," *Journal of Computational Physics*, vol. 242, pp. 351–366, 2013.

[28] Z. N. J. and K. M. D., "Interaction of solitons in a collisionless plasma and the recurrence of initial states," *Physical Review Letters*, vol. 15, no. 6, pp. 240–243, 1965.

Jin-liang Yan was born in Pingyao, Shanxi Province, China, in 1979. The author respectively received his Ph.D. and Master's degrees in computational mathematics at Nanjing Normal University, Nanjing, Jiangsu Province, China, in July 2016 and July 2010.

Now, he is a teacher of the Department of Mathematics and Computer, Wuyi University, Wuyishan, China. His research interests include structure-preserving algorithms, numerical solution of partial differential equations, and computing sciences.

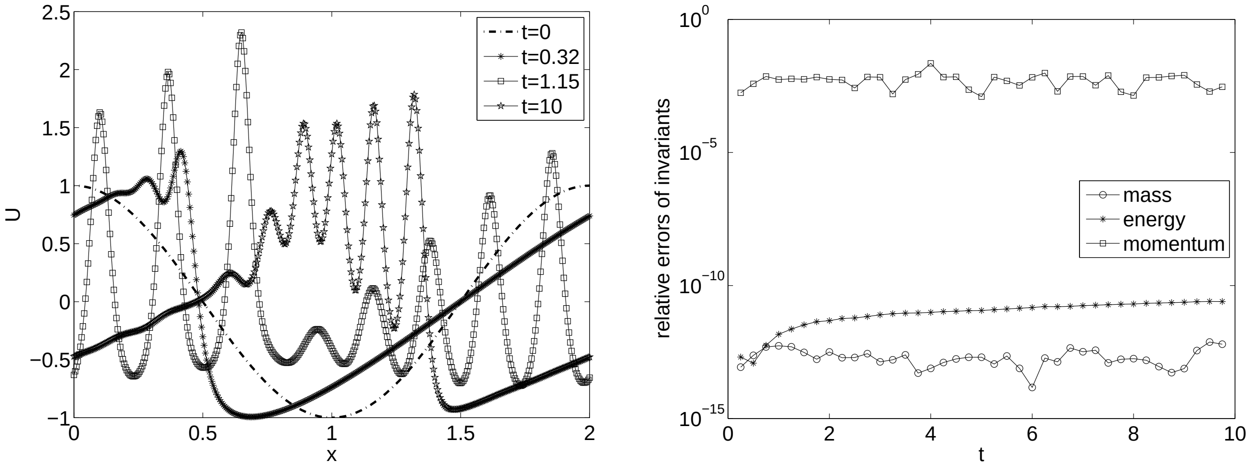

(a) (b)

Fig. 8: Numerical results of the LEFVEM at different times with $h = 1/200$ and $\Delta t = 0.01$: (a) numerical solution, (b) the relative errors of invariants.

Liang-hong Zheng was born in Nanping, Fujian Province, China, in 1983. She received her bachelor's degree in computer science and technology from Minnan Normal University, Zhangzhou, Fujian Province, China, in July 2009.

Presently, she is a teacher of the Department of Information and Technology, Nanping No. 1 Middle School, Nanping, China. Her research interests include algorithm design, artificial intelligence, robot competition, and video production.